BJ Jones, L Anguilano, JJ Ojeda ***Argon plasma treatment techniques on steel and effects on diamond-like carbon structure and delamination*** *Diamond & Related Materials* ***20*** *(2011) 1030-1035*
Archive Version. The definitive version is available at www.sciencedirect.com or via http://dx.doi.org/10.1016/j.diamond.2011.06.004

Argon plasma treatment techniques on steel and effects on diamond-like carbon structure and delamination

B.J. Jones*, L. Anguilano, J.J. Ojeda

Experimental Techniques Centre, Brunel University, Uxbridge, UB8 3PH, UK

Abstract

We demonstrate alteration in diamond-like carbon (DLC) film structure, chemistry and adhesion on steel, related to variation in the argon plasma pretreatment stage of plasma enhanced chemical vapour deposition. We relate these changes to the alteration in substrate structure, crystallinity and chemistry due to application of an argon plasma process with negative self bias up to 600 V.

Adhesion of the DLC film to the substrate was assessed by examination of the spallated fraction of the film following controlled deformation. Films with no pretreatment step immediately delaminated. At 300 V pretreatment, the spallated fraction is 8.2%, reducing to 1.2% at 450 V and 0.02% at 600V. For bias voltages below 450V the adhesion enhancement is explained by a reduction in carbon contamination on the substrate surface, from 59at.% with no treatment to 26at.% at 450V, concurrently with a decrease in the surface roughness, R_q, from 31.5nm to 18.9nm. With a pretreatment bias voltage of 600V a nanocrystalline, nanostructured surface is formed, related to removal of chromium and relaxation of stress; X-ray diffraction indicates this phase is incipient at 450V. In addition to improving film adhesion, the nanotexturing of the substrate prior to film deposition results in a DLC film that shows an increase in sp^3/sp^2 ratio from 1.2 to 1.5, a reduction in surface roughness from 31nm to 21nm, and DLC nodular asperities with reduced diameter and increased uniformity of size and arrangement. These findings are consistent with the substrate alterations due to the plasma pretreatment resulting in limitation of surface diffusion in the growth process. This suggests that in addition to deposition phase processes, the parameters of the pretreatment process need to be considered when designing diamond-like carbon coatings.

Prime Novelty: We elucidate the mechanisms behind the enhancement of diamond-like carbon film adhesion with increase in pretreatment bias voltage, and demonstrate the effect on the final film structure of alterations in the pretreatment process.

Keywords: Diamond-like carbon; plasma enhanced CVD; surface structure; delamination; morphology; interface

* Corresponding author. Tel: +44 1895 265409 / 255793 Fax: +44 1895 812544
e-mail address: b.j.jones@physics.org (B.J. Jones)

1. Introduction

Hard-wearing, low-friction, and biocompatible, diamond-like carbon (DLC) is a thin-film amorphous material that contains both sp^2 (graphitic) and sp^3 (diamond-like) bonded carbon atoms, and often a significant level of hydrogen, depending on the deposition technique. The medium-range order, clustering of the sp^2 bonded atoms within an sp^3 matrix, is also important in determining the nature and properties of the material, and the incorporation of dopants enables additional control [1-4]. Tuning the balance of the constituents, phases and ordering allows the creation of an amorphous carbon material with properties that can range from polymer-like to diamond-like. This range of materials can therefore be tailored to match functional requirements, resulting in applications in many areas including aerospace [5] manufacturing [6] and medical devices [7-10].

The potential risk of delamination of an applied diamond-like carbon film can be a concern in many applications. In the case of medical applications, the integrity of the DLC layer can be critical. A breach in a diffusion barrier coating could cause leaching of toxic metal into the body [8-10], or a breakdown in the coating on a vascular stent could lead to increased thrombogenicity due to the exposure of the underlying metal, leading to restinosis, a closing of the blood vessel [7]. Delamination debris can also be a concern. DLC is inert and biocompatible in the form of a thin film coating [11], but work on diamond-like carbon debris [12] shows fragments can be internalised by bone marrow cells, although of the DLC variants studied, an inflammation response was only shown from multilayer titanium-containing films.

Many groups producing amorphous carbon or amorphous hydrogenated carbon films use thin interlayers with incorporation of elements such as titanium [13], tungsten [14-16] or silicon [6, 7, 10, 17-19]. These layered structures have improved adhesion on substrates including stainless and high-speed steels [6, 7, 19] silicon [7, 17] and Ti-Al-V alloys [18]. Other research teams have used thick interlayers such as ceramic or epoxy [5]. Many groups [5, 6, 13, 19-22] also utilise an argon plasma pretreatment process, and this has been shown to be important in film adhesion [5, 20, 21]. However, parameters for this process vary substantially between groups; duration can vary from 5min to 1 hr and bias voltage from 300V to 700V. This paper shows the effects of the argon pretreatment process variations on stainless steel substrates and on the structure and delamination resistance of the resulting DLC film.

2. Experimental

Argon pretreatment and DLC film deposition were conducted utilising a 13.56-MHz rf-powered, capacitively coupled, plasma enhanced chemical vapour deposition (PECVD) reactor (sometimes referred to as plasma assisted, PACVD). Substrates were 304-stainless

steel (18wt% Cr, 8wt% Ni) coupons, approximately 10x10x0.5mm. The substrates were ultrasonically cleaned with acetone for 15 min and mounted within the chamber, which was then evacuated to a background pressure below 8×10^{-5} torr. An argon plasma with flow rate of 30 sccm and pressure of 8×10^{-2} torr was applied for 30min with the power controlled to achieve a negative self bias voltage from 300 V to 600 V.

Additional samples were produced utilising the same argon pretreatment process, with subsequent deposition of a multilayer DLC film. Although pretreatment bias voltages are varied, the subsequent DLC films were all produced with identical deposition conditions. Multiple samples were produced for each condition to allow subsequent analysis procedures. Following pretreatment, the bias voltage was adjusted to 450V and an interfacial layer was formed by adjusting the argon flow rate to 10sccm and introducing tetramethylsilane (TMS) with a flow rate of 25 sccm. This layer enhances the adhesion of the film to the substrate [6, 7, 19]. Once the interfacial layer was formed, the TMS gas flowing into the system was reduced to 12.5sccm, and acetylene gas at 60 sccm was introduced into the chamber to form a transition layer. The TMS was cut off and argon and acetylene flow rates and bias were maintained for the final layer deposition. The duration of deposition of each layer was 15 min, resulting in a film approximately 0.75µm thick; these parameters have been shown to produce good substrate adhesion, wear resistance and low friction coatings for machine tools [6].

Samples were removed from the reactor and examined within a Zeiss Supra 35VP field emission scanning electron microscope (SEM) operating at 1.5 - 6kV for secondary electron analysis. Surface texture parameters were assessed with a Digital Instruments DI3100 atomic force microscope (AFM) operating in tapping mode with a silicon cantilever operating at approximately 150kHz. Root mean square (RMS) roughness measurements, R_q, are calculated over 10µm square areas, and show the mean and variation over at least five regions. The XPS measurements for surface chemistry were made on a VG Escalab 210 Photoelectron Spectrometer. The X-ray source was a non-monochromated Al Kα source (1486.6eV), operated with an X-ray emission current of 20 mA and an anode high tension (acceleration voltage) of 12 kV. The takeoff angle was fixed at 90° relative to the sample plane. The area corresponding to each acquisition was a rectangle of approximately 5x2 mm. Each analysis consisted of a wide survey scan (pass energy 50eV, 1.0eV step size) and high-resolution scans (pass energy 50eV, 0.05eV step size) for component speciation. The binding energy scale was calibrated using the Au $4f_{5/2}$ (83.9 eV), Cu $2p_{3/2}$ (932.7 eV) and $Ag3d_{5/2}$ (368.27 eV) lines of cleaned gold, copper and silver standards from the National Physical Laboratory (NPL), UK. Crystallinity measurements were conducted utilising a Bruker D8 Advance X-ray diffractometer with non-monochromated copper Kα soruce (1.54056 Å) operated at 40KV and 40mA. Crystal size, texture (preferential orientation) and structure refinement were performed through Rietveld Refinement using Topas.

DLC coated steel samples were subjected to three-point bending through an angle of approximately 35^{o} and were subsequently analysed by SEM. Measurement of the spallated fraction of the film surface was calculated by analysis of three separate areas each of approximately $2.3mm^2$.

3. Results and discussion

3.1 Plasma Treatment of Stainless Steel

Figure 1 shows the variation of the steel surface with argon treatment process. Figure 1a shows the substrate with no Ar treatment, with extensive contamination. Figures 1b-1c show the substrate surface resulting from Ar treatment with bias voltage increasing from 300 V to 450 V, showing the etching process leads to removal of contaminants and increased definition of the underlying structure. A pretreatment process with a bias voltage of 600 V induces the formation of a nanostructured substrate surface, figure 1d, with clear differences in packing arrangement between different areas. This is shown more clearly in the higher magnification image figure 1f, and a nanostructured surface can be seen to begin to form after a 450V treatment (figure 1e). Atomic force microscopy measurements, summarised in table 1, show a decrease in the surface roughness (R_q) from 31.3nm to 18.9nm as the argon bias voltage of the pretreatment process is increased from 370V to 450V, this is concurrent with an increase in the kurtosis of the surface (a measure of the sharpness of peaks). With a bias of 600V the surface structure is significantly altered, the nanostructuring observed in the SEM images increases the surface roughness from 18.9 nm to 26.5 nm, the kurtosis is reduced from 7.8 to 3.3, and the number of peaks in the topography increases from approximately 316 per 10x10µm area to 2672 over the same size area.

X-ray photoelectron spectroscopy measurements show the variation in chemistry of the sample surface, with an analysis depth of approximately 10nm. Table 1 indicates the relative elemental composition of the sample surface with increasing argon bias voltage. From the lowest bias voltage of 300V, the argon process acts to remove the adventitious carbon contamination, as can be seen by the reduction in carbon content and increase in the iron content from those of the untreated steel surface. Incorporation of aluminium onto the sample surface is caused by contamination from the shielding within the PECVD reactor. As the XPS is an *ex-situ* technique, the oxygen content observed is related to sample transfer. As the treatment bias voltage is increased from 450V to 600V the chromium content of the surface is reduced from 8.0% to 1.2%, in tandem with the surface nanostructuring observed by SEM and AFM.

Analysis of the untreated sample crystallinity by X-ray diffraction shows an austenitic structure with a preferential orientation, as anticipated for 304 stainless steel, and shown in

figure 2. For argon plasma treatment at bias of 300V or 370V, the XRD spectra shows no alteration from the untreated steel, and a crystal size of approximately 200nm. As bias voltage increases to 450V, an incipient, broader, off-set peak series becomes apparent as indicated in figure 2 (inset); Rietveld refinements indicate this is related to an additional phase of crystal size 30nm. The fraction of this phase is increased at bias of 600V, where two nanostructured phases are observed. The shift of the peaks of the nanocrystalline phases from the position seen in the untreated steel is due to a combination of the alteration in unit cell size from the removal of chromium, the relaxation of residual stress and the unfocussing of the diffracted beam related to the spatial relationship of the observed phases. The crystal size is of similar dimension to the nanostructured features observed by SEM (figure 1f). The presence of multiple, off-set austenitic phases in the XRD spectrum is again consistent with the SEM image, and indicates the top nanostructured layer is of thickness less than approximately 10µm, the analysis depth of the XRD technique. The change in the ratio of intensity of peaks, at for example (002) and (022), indicates that the nanostructured phase has a less preferential crystal orientation compared to the microcrystals, which may be attributed to fast crystallisation within the boundaries created by the microcrystal.

3.2 Diamond-like carbon films on plasma treated steel

Figure 3 shows SEM images of DLC films following substrate distortion, demonstrating cracking and spallation of the film occurring with substrate bending. Variation in the damage process with increasing pretreatment bias voltage is shown in table 2. The film deposited on a substrate with no argon pretreatment, not shown, exhibits irregular deposition and immediately delaminates. Use of the argon pretreatment shows improved adhesion, with increasing bias voltage reducing the spallated fraction of film from approximately 10% at lower voltages to approaching 0.01% with a treatment at 600 V bias. This is consistent with the reduction in fracture damage seen with increasing pretreatment bias by Choi *et al.* [21]

The analysis of the treated substrate, coupled with assessment of delamination, suggests multiple processes for enhancement of film adhesion. For bias voltages 300V-450V the adhesion enhancement is explained by a reduction of contamination on the surface. As the bias voltage is increased from 450V to 600V bias the formation of a nano-structured interface with between the film and substrate further enhances the film-substrate adhesion. Unlike the spallations in films treated with Ar plasma at 300 – 450V bias, the very occasional breaches in the 600 V treated film appear to be unlinked to the crack lines, as shown in figure 3 d, and are perhaps related to isolated substrate anomalies or contamination, which have been previously shown to be responsible for lower film adhesion [13].

Figure 4 shows scanning electron microscopy images of the surfaces of diamond-like carbon films deposited on substrates with treatments at 300V, 450V and 600V. The surface structure is quantified through atomic force microscopy (AFM) measurements of surface texture parameters RMS roughness, kurtosis and peak density, summarised in table2. XPS analysis of the DLC films enabled the assessment of the sp^3/sp^2 ratio at the sample surface through a deconvolution of the C1s peak, as shown in figure 5, following the procedures described by Leung *et al.*[23] and Yan *et al.* [24]. The C1s peak was fitted with component peaks for sp^2 and sp^3 configurations, along with components for C=O, C-O and O-C=O bonded carbon [23, 24]. The line shape was assumed to be 70% Gaussian and 30% Lorentzian, and the separation of the sp^2 and sp^3 components was fixed at 0.5eV [23, 24]. Values for sp^3/sp^2 ratio are shown in table 2.

These analyses demonstrate that the argon pretreatment process has a significant effect on the DLC surface structure. Treatment at 300V (figure 4 a) leads to a DLC film with a non-uniform distribution of nodules of various sizes, from sub 100nm to over 1.5µm. Increasing the bias voltage to 450 V (figure 4 b) leads to improved uniformity of nodule size, with significantly fewer large asperities. In some areas substrate features affect the size and shape of these nodules, with machining marks becoming more prominent. Utilising a pretreatment process with a bias voltage of 600V (figure 4 c) results in a decrease in surface roughness, and smaller, more ordered asperities with increased uniformity of approximately 100nm – 200nm in diameter. The surface chemistry of the final film is also affected by the argon pretreatment process. With the development of a nanostructured substrate with increase bias voltage, the sp^3/sp^2 ratio of the final film surface increases from 1.2 at 300V and 370V, to 1.5 at 450V and 600V. There are clear boundaries between different areas, as also observed on the uncoated substrate, and the arrangement and uniformity of the DLC asperities can be related to the nanotexturing of the substrate surface. The SEM image (figure 4 c) also shows the boundaries between regions, which with the increase in bias voltage have become more prominent than machining marks, can be potential defect sites.

Previous works have shown that the nodular nature of the topography of DLC films can be affected both by deposition parameters and by substrate. These variations affect the impinging ion species and energy, and interaction with the substrate, and consequently the balance of film growth mechanisms, argon sputter and etching by diasassociated hydrogen during the deposition phase [16,17,25,26]. Jones *et al.* [17] show nodule diameter of DLC on silicon increases with argon content of the deposition precursor gases, which is correlated with an increase in sp^2 cluster size. Work of Niu *et al.* [25] on nitrided amorphous hydrogenated carbon showed a surface asperity size increasing with chamber pressure during deposition. Xu *et al.* [16] show incorporation of tungsten onto a steel substrate, to

act as an interlayer for DLC deposition, can lead to a reduction in film surface nodule diameter and an increase in sp^3 fraction.

These results can be explained by alteration in surface diffusion, affected by ion energy, argon sputter, or substrate control [16,25,26]. An increase in surface diffusion can tend to promote formation of surface nodules, with an increasingly ordered sp^2 fraction [26]. Our findings show that increasing bias voltage of argon plasma pretreatment leads to a reduction number of larger diameter of the DLC nodules, coupled with a decrease in the sp^2 fraction observed by XPS. This is consistent with the plasma treatment of the steel substrate resulting in a limitation to the surface diffusion, reducing the diameter of the observed nodules of DLC in the final film and the reducing the related surface sp^2 content.

4. Conclusions

This work shows the effect of argon plasma pretreatment techniques for deposition of diamond-like carbon films, investigating the effect of this process on stainless steel substrates and on the delamination resistance and structure of the final DLC film. Bending tests confirm earlier results [21, 22] showing increased film adhesion with increasing bias voltage of argon pretreatment, with substantial improvement after argon pretreatment with bias of 600V. For bias voltages below 450V the adhesion enhancement is explained by a reduction of carbon contamination on the surface. As the voltage is increased in this range the DLC structure becomes more regular and increasingly follows substrate structure such as machining features. At 450V treatment, a nano-structured, nano-crystalline surface layer begins to be produced, related to stress relaxation and reduction of levels of chromium in the surface layer. This nanostructured layer becomes well defined with more energetic pretreatment process at 600V bias. In addition to improving the adhesion of the film, the increase in bias voltage of the pretreatment process also affects the surface topography and chemistry of the diamond-like carbon. The nanotexturing of the substrate prior to film deposition due to an increased bias voltage results in a DLC film that shows an increase in sp^3/sp^2 ratio, a reduction in surface roughness and an increase in uniformity of size and arrangement of asperities, consistent with a limitation in surface diffusion in the growth process, in contrast to the substrates with treatment at lower bias voltages. The pretreatment process at 600V also results in additional topographical features related to substrate boundaries, which are likely to be detrimental in some applications. The alterations in the film structure are likely to have an effect on the applicability of the films across sectors [4-10] and suggest that in addition to deposition phase processes, the parameters of the pretreatment process need to be considered when designing diamond-like carbon coatings.

Acknowledgements

Grateful thanks to Prof J Franks, Brunel University, for deposition of DLC films with PECVD and to N Nelson, Brunel University, for technical assistance.

This work is partially supported by the Technology Strategy Board, reference BD266E.

References

[1] Erdemir, A and Donnet, C. Tribology of diamond-like carbon films: recent progress and future prospects *J. Phys. D: Appl. Phys.* 2006 **39:** R311

[2] Robertson, J Diamond-like amorphous carbon *Materials Science and Engineering: R: Reports* 2002; **37**: 129-281

[3] Lettington, A.H. Applications of diamond-like carbon thin films. *Carbon* 1998; **36**:555-60

[4] Jones, B.J., Barklie, R.C., Smith, G., El Mkami, H., Carey, J.D. and Silva, S.R.P. An EPR study at X- and W-Band of defects in a-C:H films in the temperature range 5K- 300K. *Diamond Relat. Mater.* 2003; **12**:116-23

[5] Podgoric, S., Jones, B.J., Bulpett, R., Troisi, G. and Franks, J. Diamond-like carbon / epoxy combination low-friction coatings to replace electroplated chromium. *Wear* 2009; **267**:996-1001

[6] Zolgharni, M., Jones, B.J., Bulpett, R., Anson, A.W. and Franks, J. Energy efficiency improvements in dry drilling with optimised diamond-like carbon coatings. *Diamond Relat. Mater.* 2008; **17**:1733-7

[7] Maguire, P.D., McLaughlin, J.A., Okpalugo, T.I.T., Lemoine, P., Papakonstantinou, P., McAdams, E.T.*, et al*. Mechanical stability, corrosion performance and bioresponse of amorphous diamond-like carbon for medical stents and guidewires. *Diamond Relat. Mater.* 2005; **14**:1277-88

[8] Jones, B. In Diamond Health: Diamond-like carbon for medical applications. *Mater. World* 2008; **16**(8):24-6

[9] Ohgoe, Y., Hirakuri, K.K., Ozeki, K. and Fukui, Y. Investigation of Diamond-Like Carbon Coating for Orthodontic Archwire. *New Diam. Front. Carbon Technol.* 2007; **17**:281-8

[10] Jones, B.J., Mahendran, A., Anson, A.W., Reynolds, A.J., Bulpett, R. and Franks, J. Diamond-like carbon coating of alternative metal alloys for medical and surgical applications. *Diamond Relat. Mater.* 2010; **19** :685–689

[11] Thomson, L.A., Law, F.C., Rushton, N. and Franks, J. Biocompatibility of Diamond-like Carbon Coating. *Biomaterials* 1991; **12**:37-40

[12] Bruinink, A., Schroeder, A., Francz, G. and Hauert, R. In vitro studies on the effect of delaminated a-C:H film fragments on bone marrow cell cultures. *Biomaterials* 2005; **26**:3487-94

[13] Moura e Silva, C.W., Alves, E., Ramos, A.R., Sandu, C.S. and Cavaleiro, A. Adhesion failures on hard coatings induced by interface anomalies. *Vacuum* 2009; **83**:1213-7

[14] Takeno, T., Sugawara, T., Miki, H. and Takagi, T. Deposition of DLC film with adhesive W-DLC layer on stainless steel and its tribological properties. *Diamond Relat. Mater.* 2009; **18**:1023-7

[15] Lee KR, Eun KY, Kim I, Kim J Design of W buffer layer for adhesion improvement of DLC films on tool steels *Thin Solid Films* 2000; **138**: 261-8

[16] Xu M, Zhao J, Cai X, Chen QL, Chu PK Structure and topographies of diamond-like carbon films produced on tungsten pre-implanted stainless steel substrate by plasma immersion ion implantation and deposition *Diamond Relat. Mater.* 2007; **16**: 1490-9

[17] Jones, B.J., Wright, S., Barklie, R.C., Tyas, J., Franks, J. and Reynolds, A.J. Nanostructure and paramagnetic centres in diamond-like carbon: effect of Ar in PECVD process. *Diamond Relat. Mater.* 2008; **17**:1629-32

[18] Chandra, L., Allen, M., Butter, R., Rushton, N., Lettington, A.H. and Clyne, T.W. The effect of exposure to biological fluids on the spallation resistance of diamond-like carbon coatings on metallic substrates. *J. Mater. Sci.: Mater. Med.* 1995; **6**:581-9

[19] Jing, W., Gui-Chang, L., Li-Da, W., Xin-Lu, D. and Jun, X. Studies of diamond-like carbon (DLC) films deposited on stainless stell substrate with Si/SiC intermediate layers. *Chinese Phys. B* 2008; **17**:3108-14

[20] Kim, H., Moon, M., Kim, D., Lee, K. and Oh, K.H. Observation of the failure mechanism for diamond-like carbon film on stainless steel under tensile loading. *Scripta Mater.* 2007; **57**:1016-9

[21] Choi, H., Lee, K., Wang, R. and Oh, K.H. Fracture behavior of diamond-like carbon films on stainless steel under a micro-tensile test condition. *Diamond Relat. Mater.* 2006; **15**:38-43

[22] Marciano, F.R., Bonetti, L.F., Da-Silva, N.S., Corat, E.J. and Trava-Airoldi, V.J. Wettability and antibacterial activity of modified diamond-like carbon films. *Appl. Surf. Sci.* 2009; **255**:8377-82

[23] Leung, T.Y., Man, W.F., Lim, P.K., Chan, W.C., Gaspari, F., Zukotynski, S. Determination of the sp3/sp2 ratio of a-C:H by XPS and XAES, *Journal of Non-Crystalline Solids* 1999; **254**: 156-160

[24] Yan, X.B., Xu, T., Yang, S.R., Liu, H.W., Xue, Q.J. Characterization of hydrogenated diamond-like carbon films electrochemically deposited on a silicon substrate *J. Phys. D: Appl. Phys.* 2004; **37**: 2416–24

[25] Niu JH, Zhang LL, Zhang ZH, Liu DP, Liu YH, Feng ZQ Deposition of hydrogenated amorphous carbon nitride films by dielectric barrier discharge plasmas *Appl. Surf. Sci.* 2010; **256**: 6887-92

[26] Peng XL, Barber ZH, Clyne TW Surface roughness of diamond-like carbon films prepared using various techniques *Surf. Coat. Technol.* 2001; **138**: 23-32

Figures & Tables

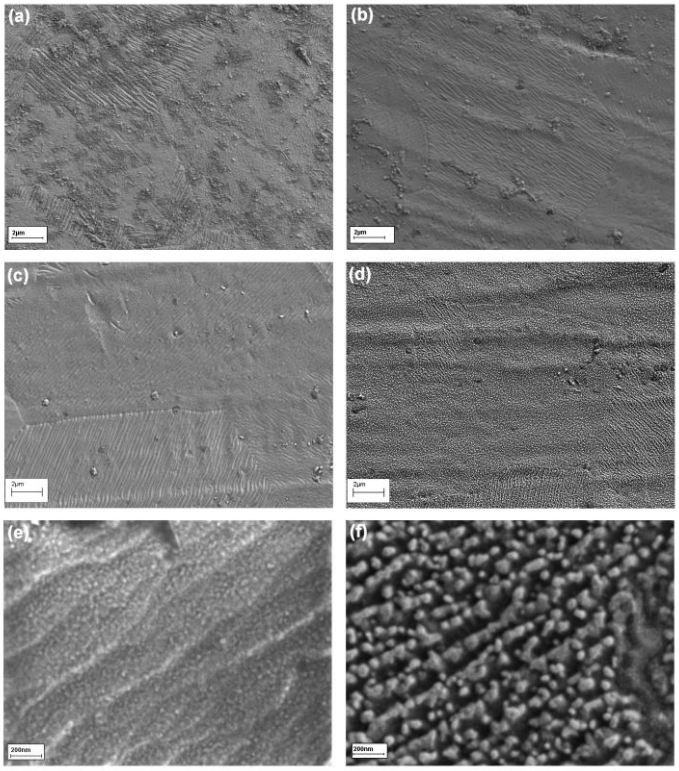

Figure 1: SEM images of stainless steel substrates (a) sonication preclean only; and additional argon pretreatment with bias voltages of (b) 300V (c) 450V (d) 600V. Higher magnification images of the surface after pretreatment at (e) 450V and (f) 600V.

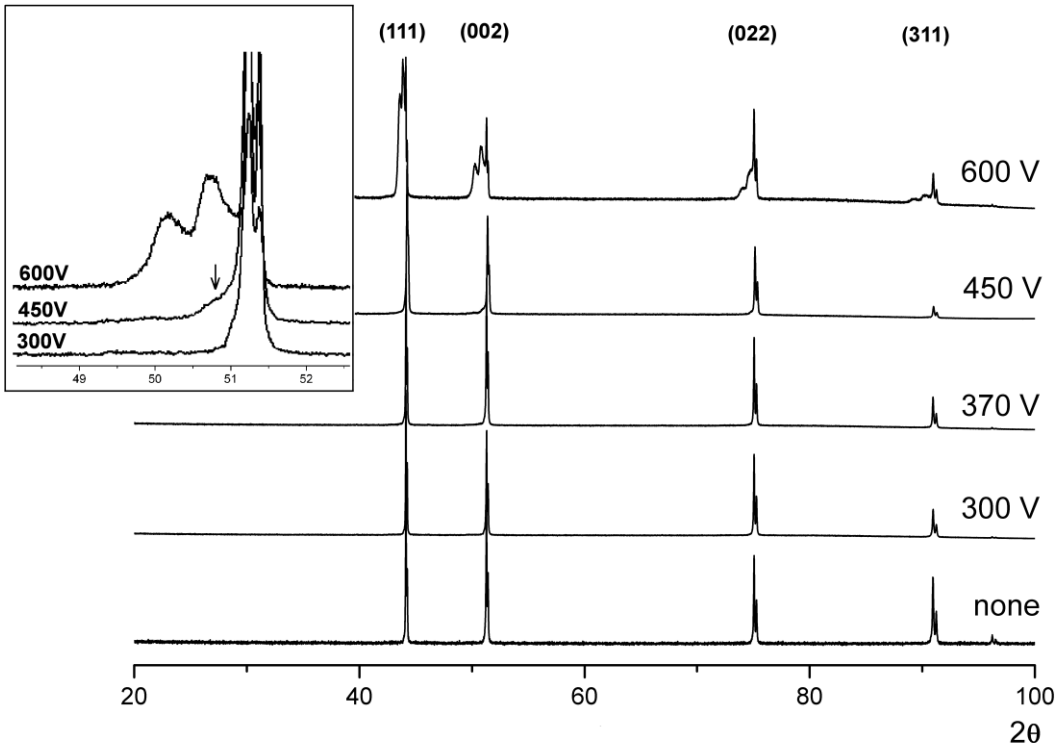

Figure 2: X-ray diffraction spectra for plasma treated stainless steel with pretreatment bias voltages to 600V. Inset shows enlargement of peaks at 49<2θ<52, with the nanostructured phase initiating in the sample treated at 450V (indicated) and becoming more defined at 600V.

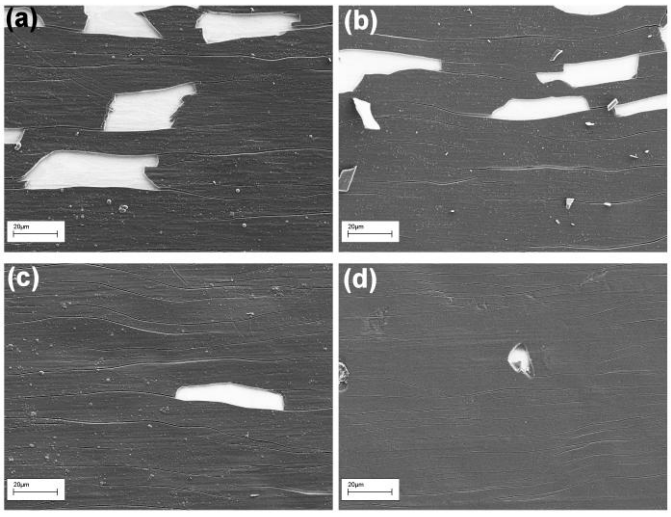

Figure 3: Scanning electron microscopy images showing DLC films following bend testing, demonstrating cracking and spallation of films produced with Ar pretreatment process at bias voltages of (a) 300V (b) 370V (c) 450V (d) 600V

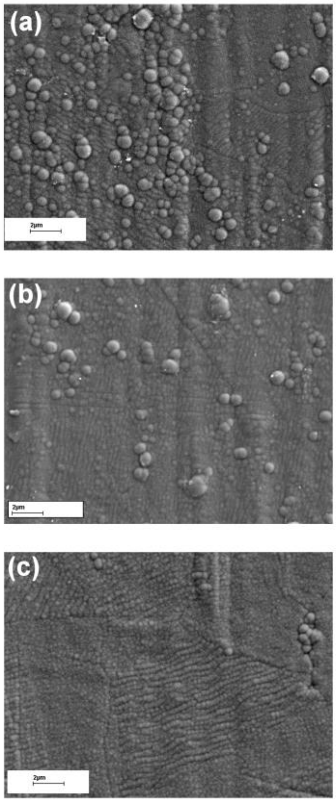

Figure 4: Scanning electron microscopy images of DLC films deposited on substrates with Ar pretreatment at bias voltages of (a) 300V (b) 450V and (c) 600V

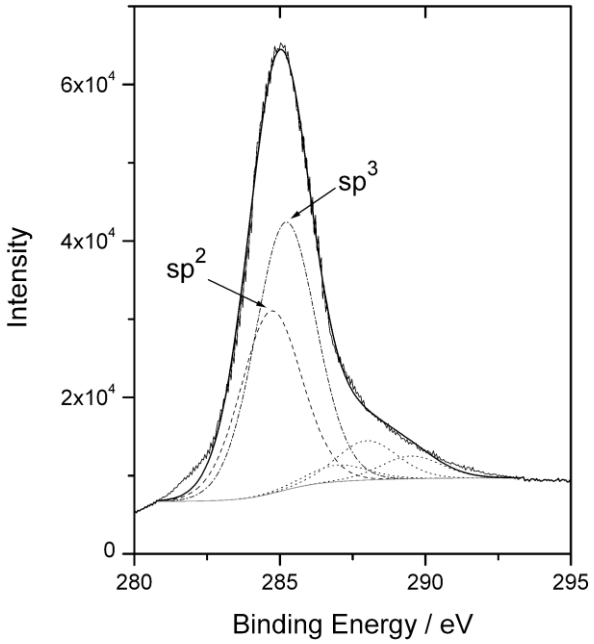

Figure 5: XPS spectrum of C1s line for DLC on stainless steel plasma treated at 600V, showing deconvolution into components.

Plasma Treatment Bias Voltage	Fe / at.%	Cr / at.%	C / at.%	O / at.%	Al / at.%	Rq / nm	Kurtosis	Peaks /100μm^{-2}
None	2.0	1.4	59.4	28.9		31.5±3.3	3.0±0.5	367±73
300	4.0	7.6	41.6	40.1	5.2	28.5±1.8	3.3±0.7	145±31
370	6.8	9.9	28.0	47.2	6.2	31.3±2.4	2.8±0.4	170±57
450	8.5	8.0	26.1	50.5	5.2	18.9±3.5	7.8±1.7	316±104
600	12.9	1.2	28.6	52.7	1.8	26.5±6.6	3.3±0.2	2673±820

Table 1. Surface structure of plasma treated 304 stainless steel, assessed by XPS and AFM

Plasma Treatment Bias Voltage	sp^3/sp^2	Rq / nm	Kurtosis	Spallated fraction
None	No adherent film			
300	1.2	37.1±6.0	3.3±1.1	8.2±1.5
370	1.2	31.0±6.7	3.1±0.3	12.4±1.8
450	1.5	29.4±3.7	2.8±0.2	1.21±0.7
600	1.5	20.9±3.7	4.5 ±0.3	0.02±0.01

Table 2. Surface structure and film delamination of DLC on plasma treated 304 stainless steel, assessed by XPS, AFM and SEM.